

DAER to Reject Seeds with Dual-loss Additional Error Regression

Stephan J. Lemmer
Robotics Institute
University of Michigan
Ann Arbor, USA
lemmersj@umich.edu

Jason J. Corso
Electrical Engineering and Computer Science
Robotics Institute
University of Michigan
Ann Arbor, USA
jjcorso@umich.edu

Abstract

Many vision tasks require side information at inference time—a seed—to fully specify the problem. For example, an initial object segmentation is needed for video object segmentation. To date, all such work makes the tacit assumption that the seed is a good one. However, in practice, from crowd-sourcing to noisy automated seeds, this is not the case. We hence propose the novel problem of seed rejection—determining whether to reject a seed based on expected degradation relative to the gold-standard. We provide a formal definition to this problem, and focus on two challenges: distinguishing poor primary inputs from poor seeds and understanding the model’s response to noisy seeds conditioned on the primary input. With these challenges in mind, we propose a novel training method and evaluation metrics for the seed rejection problem. We then validate these metrics and methods on two problems which use seeds as a source of additional information: keypoint-conditioned viewpoint estimation with crowdsourced seeds and hierarchical scene classification with automated seeds. In these experiments, we show our method reduces the required number of seeds that need to be reviewed for a target performance by up to 23% over strong baselines.

1. Introduction

Many tasks in computer vision require not only a *primary input*, such as an image or video, but also a secondary input—a *seed*. This seed may be used to define the problem, such as in visual object tracking [25], visual object segmentation [27], and visual question answering [1], or to provide additional information for tasks such as hierarchical scene classification [24], multi-label image classification [39], or keypoint-conditioned viewpoint estimation [36].

The performance of computer vision models with poor primary inputs has been explored in the context of naturally

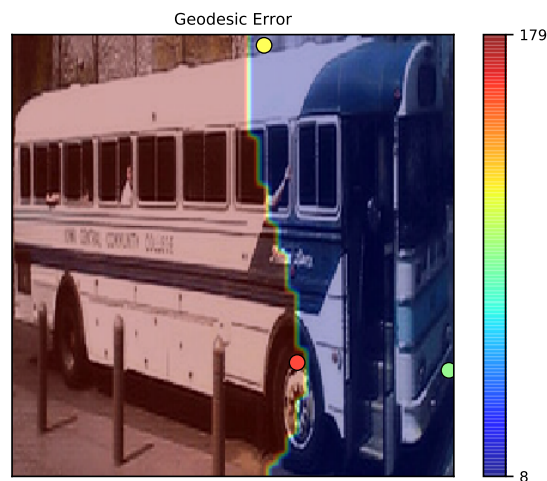


Figure 1: When determining whether or not to accept a seed, the decision must take into account not only how close the seed is to the correct seed (green) but also the characteristics of the model and image. A seed that is closer to correct in the input space (red) might significantly increase the error, while a seed significantly further away (yellow) may not.

difficult [38, 44, 6, 12] and intentionally adversarial [40, 41, 7, 35] primary inputs, leading to a variety of methods designed to make models more robust [38, 44] or detect and reject difficult inputs [12].

While some work has focused on obtaining better seeds through choosing what information to request from an annotator [15, 2], no work to our knowledge has been performed on the identification and rejection of seeds which cause a significant increase in error on the task. This is a critical oversight, as seeds are likely to be unreliable in unpredictable ways. The reliability—or lack thereof—of crowdsourced seeds is well studied [22, 28, 32, 31], and while modern deep learning systems are continuously push-

ing boundaries, they are still subject to counterintuitive failure modes [30].

In this work, we begin to resolve this critical oversight by directly studying the problem of seed rejection. In seed rejection, we seek to reject seeds that significantly degrade the performance of the *task model*, which estimates the target value based on the primary input and seed. Seed rejection introduces two unique challenges:

Understanding the Cause of Error: The first challenge is distinguishing between poor outputs due to poor seeds and poor outputs due to poor primary inputs. If the source of the error is the primary input (Figure 2b), little benefit would be obtained from requesting another seed. While the task of selective prediction has been proposed for handling bad primary inputs, no work to our knowledge has been performed on the task of rejecting bad seeds independent of the quality of the primary input.

Understanding the Task Model Response: Next, we must gain an understanding of the model’s response, and how a human’s intuition of a seed’s quality differs from its effect on the accuracy of the model’s output. For example, in Figure 1, we see that a very small Euclidean error in the input space can induce a significant increase in error in the output space, while a much smaller Euclidean error can have little effect. Similarly, the model may have very strong priors based solely on the primary input, which means it will ignore the—potentially noisy—additional information that is provided by the seed (Figure 2a).

We address these challenges via Dual-loss Additional Error Regression (DAER), a novel training method developed for the seed rejection problem. DAER considers the two challenges discussed above separately, and combines them to produce an estimate for the effect of the seed on the downstream task.

To compare DAER to baselines, we introduce three novel metrics: Additional Error (AE), Mean Additional Error (MAE), and Area under the Mean Additional Error curve (AMAE). Instead of simply measuring the error of accepted samples like previous metrics [13], these three metrics measure how much error in the accepted samples can be corrected by obtaining the correct seed.

We evaluate the performance of the proposed method and metrics on two separate tasks, both of which use the seed to provide additional evidence: keypoint-conditioned viewpoint estimation [36] and Plugin Networks for hierarchical scene classification [24]. In addition, we develop further understanding of task model’s response to incorrect seeds on both these tasks through an exhaustive sampling. As models which use this strategy universally assume that this information is correct this is, to our knowledge, the first instance of such an analysis.

The contributions of this paper are as follows:

1. Introduction and definition of the seed rejection prob-

lem.

2. The metrics of Additional Error (AE), Mean Additional Error (MAE) and Area under the Mean Additional Error curve (AMAE) for evaluating the task of seed rejection.
3. Dual-loss Additional Error Regression (DAER): A novel training and inference method for seed rejection.
4. An exhaustive sampling of the response of the both task models to incorrect seeds, justifying the use of DAER over direct regression.

2. Related Work

2.1. Seeded Inference

Seeded inference describes a number of problems in which a primary input and a seed are provided at inference time to estimate a target. Broadly speaking, the seed can be categorized across two axes: The first axis is whether the seed is provided by a human [3, 33] or a separate automated system [14, 29]. The second is whether the seed is used to fully define the task, such as initial bounding boxes for single-target object tracking [25], or used to further inform the inference—sometimes referred to as “inference under partial evidence” [39]. In this work, we consider both crowdsourced and automated sources of this additional information through two tasks: keypoint-conditioned viewpoint estimation [36] and hierarchical scene categorization [24, 39, 19].

In general, whether the seed is used to define the task or to provide extra information is easy to determine. For example, the tasks of video object segmentation [27], single-target tracking [25], and others [1, 21, 20] are clear cases in which the problem is not fully defined until inference time, while in cases such as keypoint-conditioned viewpoint estimation [36], hierarchical scene classification [24], multi-label image annotation [23], and visual concept prediction [39], a model could achieve better than random performance without the benefit of the seed. However, determining the mechanism through which the model obtains the seed is often less clear. In some cases the use-case is specified by the problem, such as visual question answering [1] which processes questions posed by humans, or visual servoing based on object segmentations [14] which uses an automatic segmentation method.

In other cases, the algorithm simply asserts that the seed exists, making it difficult to know the intended use. Challenges in the video space [25, 27] typically just say that the first frame is given, while many methods which use seeds to provide additional information [24, 39, 19] simply use the gold-standard for both training and inference. We note that regardless of the method used to provide the seed, it is assumed that the seed is true.

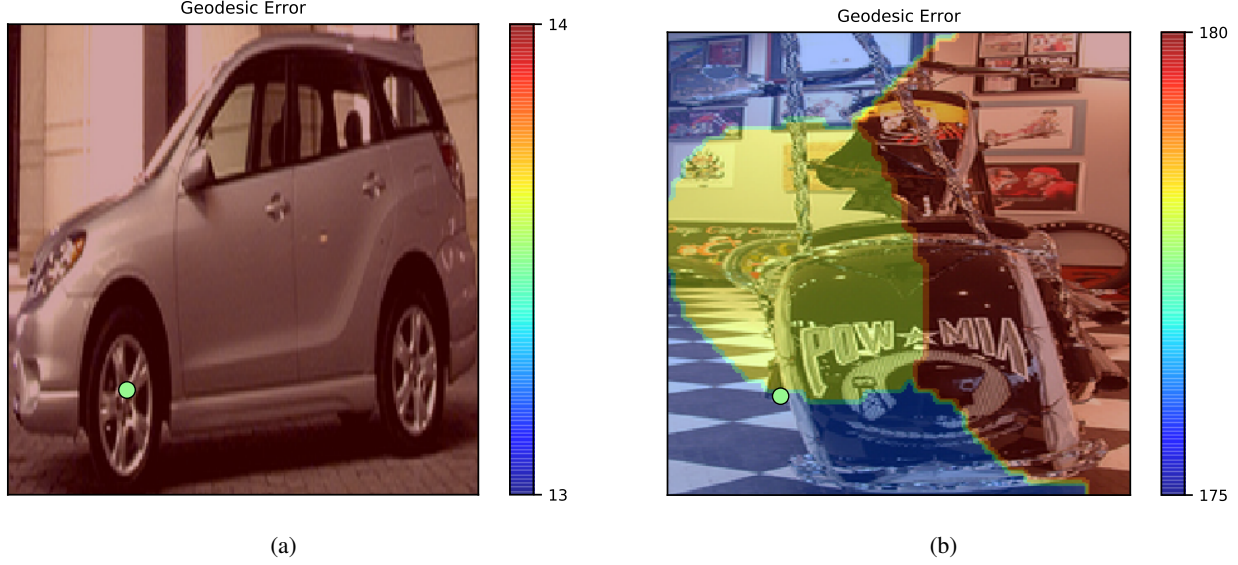


Figure 2: In many cases, the task network conditions strongly enough on the primary input that the it will either perform well (2a) or poorly (2b) regardless of the quality of the seed.

2.2. Selective Prediction

A problem closely related to seed rejection is the problem of selective prediction [4, 12], which does not consider the effects of seeds, but guesses whether a model is likely to provide the correct answer based on the primary input. Selective prediction has been applied to many approaches over time, from nearest neighbors in the 1970’s [18], to support vector machines in the early 2000s [8], to deep artificial neural networks today [43, 12].

Recent literature focuses on extending selective prediction to deep networks, though approaches vary. Yildirim et al.[43] perform mixed integer programming on dropout neural networks to build a binary classifier that takes into account not only accuracy, but also the cost of a misclassification. Geifman & El-Yaniv [11] show softmax response is a superior rejection mechanism to Monte Carlo dropout [9] in multi-class classification, and develop an algorithm which guarantees risk will fall below a certain threshold. In later work, they introduce SelectiveNet, which, much like work done in support vector machines [8], notes that performance is better if rejection is defined during training, and includes the reject option as part of its architecture [12].

3. Seed Rejection

3.1. Problem Statement

In seed rejection, we attempt to reject seeds which cause a significant increase in error when compared with a gold-standard seed. Formally stated, we begin with a task model,

$f(x, s)$ which accepts a primary input, x , and a candidate or gold-standard seed, $s \in \{s_c, s_{gs}\}$. We seek to develop a rejection model, $g_\theta(x, s_c) \in 0, 1$ which accepts a certain proportion (coverage, c_d) of candidate seeds used for inference such that the performance of the accepted set most closely matches the performance of the corresponding (unknown) gold-standard seeds.

We refer to the per-sample performance degradation as *additional error*, which is calculated:

$$AE(x, s_c, s_{gs}, y|f, \ell) = \max(\ell(f(x, s_c), y) - \ell(f(x, s_{gs}), y), 0) \quad (1)$$

where y represents the target value and ℓ represents a problem-specific performance measure. We note that the max operator ensures that the model is never penalized for accepting the gold-standard seed over a candidate seed that is incorrect in input space. With this definition of performance degradation, the problem of seed rejection for a desired coverage can be treated as finding an approximate solution to the optimization problem:

$$\begin{aligned} \arg \min_{\theta} \quad & \sum_{(x, s_c, s_{gs}, y) \in \mathcal{D}} g_\theta(x, s_c) AE(x, s_c, s_{gs}, y|f, \ell) \\ \text{such that} \quad & \frac{1}{|\mathcal{D}|} \sum_{(x, s_c) \in \mathcal{D}} g_\theta(x, s_c) = c_d \end{aligned} \quad (2)$$

where \mathcal{D} represents the set of all samples.

3.2. Metric

While the additional error metric proposed in the previous section provides a measure for the quality of a single seed, it does not provide a meaningful way to compare different rejection methods across a full dataset. In this section, we introduce the Mean Additional Error (MAE) and Area under the Mean Additional Error curve (AMAE) metrics, which can be used to compare methods side-by-side across a dataset.

As the name implies, the mean additional error corresponds to the mean additional error of all accepted samples:

$$MAE(f, g_\theta | D, \ell) = \frac{\frac{1}{|D|} \sum_{(x, s_c, s_{gs}, y) \in \mathcal{D}} g_\theta(x, s_c) AE(x, s_c, s_{gs}, y | f, \ell)}{\frac{1}{|D|} \sum_{(x, s_c) \in D} g_\theta(x, s_c)} . \quad (3)$$

While the mean additional error metric indicates which rejection model performs better at a given coverage, performance at a single coverage does not evaluate the true performance of a rejection model. In order to produce a single value with which to compare different rejection models, we produce a plot of mean additional error vs. coverage, and calculate the area underneath. We refer to this as the Area under Mean Additional Error curve (AMAE), which is found empirically using the equation:

$$AMAE = \frac{1}{|D|} \sum_{i=1}^{|D|} \frac{AE(x^i, s_c^i, s_{gs}^i, y^i | f, \ell)}{i} . \quad (4)$$

As with the MAE, a lower AMAE indicates better performance.

3.3. Method

We approach the task of seed rejection by attempting to regress the additional error. This approach is conceptually similar to Gurari et al. [16], who applied a series of hand-crafted features to predict the intersection-over-union of segmentations generated by various methods. While using qualities of the output, such as the value of a softmax output, to estimate the how likely it is that a classification is correct is an approach that is also used in selective prediction [11], this method is generally outperformed by methods specifically designed to predict how correct an answer is [8, 12].

For this reason, we perform seed rejection by attempting to regress the additional error directly through the training procedure shown in Figure 3. Critical to this training procedure is the separation of the additional error regression into two components corresponding to the challenges described in the introduction. The correctness loss, which addresses

the challenge *understanding the cause of error*, is a classifier which determines the likelihood that seed is correct. The regression loss, which addresses the challenge *understanding task model response*, regresses the additional error given that the seed is incorrect. That is, the regression loss is only updated when the given seed is incorrect.

Mathematically, the correctness and regression outputs can be used to calculate the expected additional error using the formula:

$$\begin{aligned} \mathbb{E}(AE(x^i, s_c^i, s_{gs}^i, y^i | f, \ell)) = \\ p(\text{seed_correct})(AE | \text{seed_correct}) + \\ p(\neg \text{seed_correct})(AE | \neg \text{seed_correct}) . \end{aligned} \quad (5)$$

Since the additional error for the correct seed is always zero, the formula reduces to:

$$\begin{aligned} \mathbb{E}(AE(x^i, s_c^i, s_{gs}^i, y^i | f, \ell)) \\ = p(\neg \text{seed_correct})(AE | \neg \text{seed_correct}) . \end{aligned} \quad (6)$$

We use this calculation when predicting the additional error at inference time, but this formulation is not used during training. While the chosen method of separately learning the correctness and regression outputs is mathematically equivalent to regressing the additional error directly, we show in Section 5.2 that separating the two components significantly improves performance, and in Section 6 propose a reason why this is the case.

4. Experimental Setup

Application of the generic method to a specific problem domain requires only problem specific definitions of a correct seed, error performance measure, and architecture. In this section, we demonstrate the versatility of our method by showing state-of-the-art performance on two disparate tasks: keypoint-conditioned viewpoint estimation and hierarchical scene classification.

4.1. Keypoint-Conditioned Viewpoint Estimation

In the task of keypoint-conditioned viewpoint estimation [36], a human annotator is given an image of a vehicle, and asked to click a keypoint such as “front right tire”. This human-produced information is then combined with features from a convolutional neural network to produce a more accurate estimate of camera viewpoint than would be possible without the keypoint [34, 37].

We use the “click-here CNN” model from the work by Szeto & Corso as our task model. This model accepts a scaled image crop, keypoint class, and downsampled map giving the Chebyshev distance from every pixel to the seed keypoint, and produces nine 359-bin softmax outputs. The

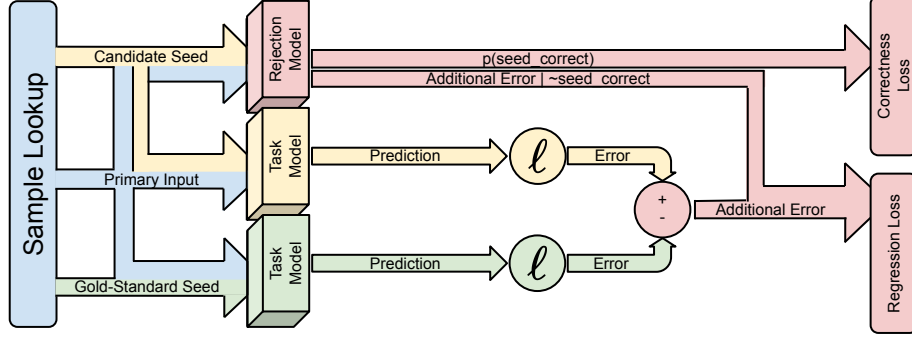


Figure 3: DAER frames seed rejection as the task of regressing the additional error, and separates the regression into two components: predicting whether the candidate seed is correct, and predicting the difference in performance between the candidate seed and the true seed given that the candidate seed is incorrect.

nine bins are conceptually grouped into three sets of three, with a 359-bin regression performed for azimuth, elevation, and tilt for each of the three vehicle classes in the PASCAL3D+ [42] dataset.

For our rejection model, we use a modified version of the click-here CNN architecture, which has been proven capable of integrating keypoint and image information. We add two additional linear layers to produce 34 sets of 201 outputs. Every set of outputs represents one of the keypoint classes. Of the 201 outputs, one is used as a binary classifier to determine whether or not the given keypoint is correct and is trained with a binary cross-entropy loss, and the other 200 are used as a classifier for determining the magnitude of error and are trained with a cross-entropy loss.

4.1.1 Training

For training, the performance measure, ℓ , is the rotation displacement formula proposed by Larochelle et al. [26]:

$$d = \|I - A_2 A_1^T\|_F. \quad (7)$$

This metric is upper bound at $2\sqrt{2}$, meaning that we divide our 200 regression output bins between $-2\sqrt{2}$ and $2\sqrt{2}$.

Since the correct answer in the input space is a single pixel, producing a classifier capable of accurately determining whether a given keypoint matches the true keypoint is a difficult task all by itself. Even given a perfect classifier, the low probability of selecting the correct gold-standard seed means the problem reduces to regressing the additional error directly.

Instead, we define a correct seed as a seed for which the additional error is zero:

$$p(\text{seed_correct}) = \begin{cases} 0 & A.E. = 0 \\ 1 & A.E. \neq 0 \end{cases}. \quad (8)$$

Aside from allowing an easier regression problem while maintaining the mathematical foundation of our method, we

believe this will help the correctness classifier view the image more holistically, classifying images such as Figures 2a and 2b as having no additional error regardless of the location of the given seed.

We train in two stages. In the first stage, we use the synthetic [34, 36] and real data together, and perform early stopping on the validation loss with patience 5. In the second stage, we train exclusively on the PASCAL3D+ dataset [42] and perform early stopping on the validation loss with patience 100.

The correctness loss is calculated using binary cross-entropy, while the regression loss is calculated using cross-entropy. Candidate seeds are generated by randomly sampling a pixel within the image.

4.1.2 Evaluation

For our evaluation, we focus on the case in which a keypoint is provided through crowdsourcing, by collecting annotations on Amazon Mechanical Turk through the provided keypoint annotation interface. A total of 6,042 gold standard keypoints were collected on the PASCAL3D+ validation set [42]. Of these keypoints, 6.3% (381) cause additional error, while 1.3% cause more than 5° additional error, and 0.5% (30) cause more than 150° additional error. We place this holdout set into 5 splits, using four for validation and one for testing for each trained network, and report the mean result.

We also change our performance measure between the training and evaluation steps. While we use a metric based on the distance from the identity matrix during training for computational reasons, we use the geodesic on the unit sphere for our evaluation. This follows the convention of previous viewpoint estimation work [36, 37, 34], and can be calculated:

$$d = \|\log(A_2 A_1^T)\|_2. \quad (9)$$

To calculate the expected additional error, we calculate the mean of the predicted additional error, and multiply it by the probability that the seed is incorrect:

$$\mathbb{E}(AE) = p(\neg \text{seed_correct}) \sum_{(x|x < 200, x \in \mathbb{N})} x(p(AE = x | \neg \text{seed_correct})) . \quad (10)$$

4.1.3 Baselines

Our baseline scoring functions for seed rejection on the keypoint-conditioned viewpoint estimation task are:

- **Known Distance:** We score the seed based on oracle knowledge of its distance from the gold-standard keypoint.
- **Task Network Entropy:** The distributional entropy of the output of Click-Here CNN. This was proposed by Gal [9] as a method of analyzing uncertainty when Monte Carlo dropout was applied to a classification task.
- **Task Network Percentile:** 10,000 weighted samples are taken from the output of Click-Here CNN. We find the absolute difference between every sample and the mean of all samples, and take the (best-performing) 80th percentile for our evaluation.
- **Softmax Response (S.R.):** The largest value of the softmax output. This has been shown by Geifman & El-Yaniv to [11] outperform the Monte-Carlo dropout [10] on selective prediction for classification tasks.

4.2. Hierarchical Scene Classification

In hierarchical scene classification, a coarse scene categorization is used to help a classifier determine the fine-grained scene classification of an object. This task was used for evaluating the role of partial evidence by Hu et al. [19], Wang et al. [39], and Koperski et al. [24].

In this work, we use the recent Plugin Network architecture developed by Koperski et al. [24] as our task model. This work applies adjustments to intermediate layers of a frozen base model based on the provided coarse categories. Through this process, they were able to use the partial evidence to increase the performance of the base model by over 4%.

4.2.1 Training

For the task of hierarchical scene classification, the performance measure is whether or not the predicted fine-grained classification matches the target fine-grained classification:

$$\ell(f(x, s)) = \begin{cases} 0 & f(x, s) = y \\ 1 & f(x, s) \neq y \end{cases} . \quad (11)$$

Since the number of coarse categories is low, we use the output of a coarse scene classifier as our correctness probability. As a backbone for our rejection model, we use a ResNet-18 [17] model pretrained on ImageNet [5], of which we use 14 outputs. 7 of those outputs represent a categorical classifier which predicts the correctness for each potential combination, while the other 7 represent the conditional additional error for each class. The two outputs are trained using cross-entropy and binary cross-entropy respectively.

The rejection model is trained for 50 epochs at a learning rate of $1e^{-5}$, and the instance with the lowest validation AMAE is used for testing.

4.2.2 Evaluation

For the hierarchical scene classification task, we use a separate coarse scene classification model to produce the seed. This allows us to test the much larger SUN-397 dataset across multiple instances of both the seeding and rejection models to calculate the standard error.

Like the rejection model, the coarse scene classification model begins with an ImageNet-pretrained ResNet-18 architecture. This classifier is trained for 20 epochs to predict one of the 7 coarse category combinations. The highest validation accuracy is used to seed the task model.

We train five rejection models and five seeding models, for a total of 5 runs on the baselines and 25 runs on learned rejection to calculate the standard error of the mean across our various rejection models.

4.2.3 Baselines

As our baselines, we use the task network entropy and softmax response as described in the hierarchical scene classification section. We perform these baselines on both the output of the task model and the output of the model which estimates the coarse classification. In our results, we refer to these as “fine” and “coarse” respectively.

5. Results

5.1. Overall Performance

In Table 1, we see the overall performance of our learned method against baseline methods on both the Keypoint-Conditioned Viewpoint Estimation (KCVE) and Hierarchical Scene Classification (HSC) tasks. We see that in both cases, the trained seed rejection method outperforms the baselines in the AMAE metric. In the case of hierarchical scene classification, we were able to train multiple coarse

Task	Method	AMAE
KCVE	Distance	0.3964
	Softmax Response	0.9292
	Entropy	0.3533
	Sampler	0.3091
	DAER	0.2864
HSC	Entropy (Fine)	$0.033 \pm 3.8e^{-4}$
	Entropy (Coarse)	$0.017 \pm 4.8e^{-4}$
	S.R. (Fine)	$0.033 \pm 3.7e^{-4}$
	S.R. (Coarse)	$0.018 \pm 4.1e^{-4}$
	DAER (Ours)	$0.016 \pm 3.3e^{-5}$

Table 1: Based on our AMAE metric, DAER outperforms baselines on both example tasks.

classifiers and DAER models to establish significance between the results.

While the mean additional error results in a meaningful summary of performance across all potential coverage, we can build better intuition by examining comparing the mean additional error at specific coverages. We examine the results from the hierarchical scene classification task more closely in Figure 4 and Table 2.

We see in the MAE-Coverage curve shown in Figure 4 that DAER outperforms all baselines after a crossover point at a coverage of 0.197. At this crossover point, the MAE is approximately 0.0045, meaning in 1 out of every 222 samples an incorrect answer will be caused by an incorrect seed.

We also show the percentage of samples which are accepted at several mean additional errors in Table 2. In the

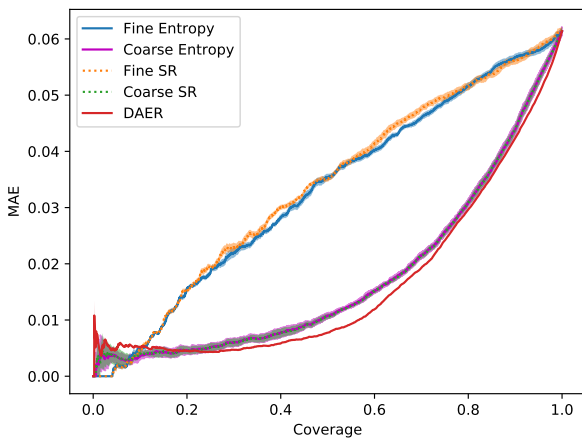


Figure 4: The additional error risk compared to the coverage for the hierarchical scene classification task. The dark line represents mean of all runs. The shaded area represents one standard error.

MAE	% Seeds Accepted (Coverage)				
	Fine Ent.	Coarse Ent.	Fine S.R.	Coarse S.R.	DAER
0.01	15.6%	48.3%	15.0%	48.2%	56.4%
0.025	35.7%	74.4%	33.0%	74.3%	75.8%
0.05	77.3%	93.3%	75.8%	93.3%	94.9%

Table 2: For a target MAE in the hierarchical scene classification task, DAER allows more seeds to be accepted without review.

case of hierarchical scene classification, a target MAE of 0.01 means that one out of every hundred fine-grained scene classifications are incorrect due to an incorrect coarse classification. At a desired MAE of 0.01, the 8.2% improvement in acceptance rate results in a 15.8% reduction in number of samples which will need to be annotated, while at a desired MAE of 0.05, the 1.6% improvement in acceptance rate results in a 23.9% reduction in number of samples which will need to be annotated.

5.2. Ablation

In this section, we justify the decision to separate our mean additional error into two separate components through use of an ablation. Here we consider separately the correctness score and the additional error regression. The additional error regression was trained on all samples regardless of whether or not the seed was correct, making it equivalent to regressing the additional error directly. No changes were made to the training of the correctness score. The results of this are shown in Table 3.

We see in these results that while the model trained to directly regress the additional error and DAER both attempt to regress the additional error, there is a significant increase in performance when the additional error is regressed conditionally on the seed being correct.

Further, we see that the correctness score is an excellent seed rejection method on its own. This indicates that the network has an easier time separating seeds that are correct from seeds that are incorrect than learning the model’s response to every particular seed—particularly when the additional error is strongly biased toward zero.

	Regression	Correctness	DAER
KCVE	1.2544	0.2937	0.2864
HSC	$0.021 \pm 1.1e^{-4}$	$0.018 \pm 1.9e^{-4}$	$0.016 \pm 3.3e^{-5}$

Table 3: Both regression and correctness contribute to overall performance, but correctness is the more significant contributor.

6. Sensitivity Analysis

As shown in the ablation, solving seed rejection as a two-part problem performs better on the final task despite being

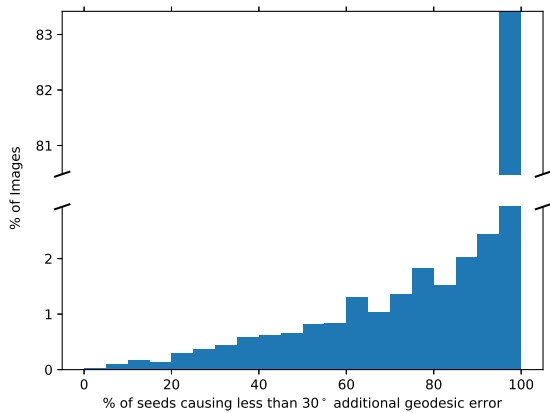


Figure 5: The sensitivity of images in the PASCAL3D+ val set to seed location. The majority of images have few potential seeds capable of causing significant error.

mathematically equivalent to directly regressing the additional error. In fact, simply building a model to ask whether or not the given evidence is correct outperforms directly regressing the additional error by a large margin. To develop an understanding of this phenomenon, we ask the previously unasked question: *what happens when the evidence we give our model is incorrect?*

We show one case where the seed significantly affects the task model’s output in Figure 1 and two cases where the task model’s output is largely unaffected by the seed in Figure 2, but to provide an overall understanding, we exhaustively sample the validation set for both our problems—that is, we provide all potential keypoint clicks in the keypoint-conditioned viewpoint estimation problem and all coarse-grained classifications for every image in the hierarchical scene classification problem. The results are seen in Figure 5 for keypoint-conditioned viewpoint estimation and Figure 6 for hierarchical scene classification.

We see that in both of these tasks the seed is often ignored, with the model instead opting to use the image as the sole source of evidence. In other words, the model has a very strong prior for some images. Specifically, we see that in the keypoint-conditioned viewpoint estimation task 78.8% of the validation dataset has no potential clicks that will increase error by more than the 30° threshold used to designate a correct regression in previous work. Further, on 83.4% of images, a random click has less than a 5% chance of increasing geodesic error by more than 30°, and 36.3% of crops do not respond to the keypoint click at all. In the case of hierarchical scene classification, 71% of images do not have any coarse classifications that cause the fine-grained classification to become incorrect.

This, alongside the results of our ablation, suggests that

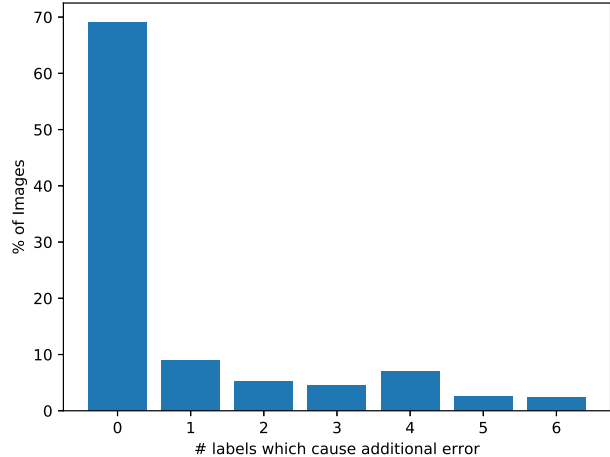


Figure 6: For 71% of images, an incorrect seed does not result in a correct fine-grained classification becoming incorrect.

while it would be possible to solve the problem by regressing additional error directly, it is a task that is subject to a very strong local minima at zero additional error. Separating the two elements allows the rejection model to first solve an easy task, such as determining whether an image is closer to Figure 1 or the examples shown in Figure 2, to accept all the seeds that are correct first, then solve the harder problem of determining the additional error of a seed on a primary input such as Figure 1 using a more balanced training signal.

7. Conclusion

In this work we have introduced the problem of seed rejection, asking what happens when the seed given to a task model is incorrect. We discuss the challenges of understanding the cause of error and understanding the task model response, then propose novel metrics for evaluating the seed rejection problem.

With these challenges and metrics in mind we propose the DAER model, which separates the task of regressing additional error into two components: predicting the correctness of the seed, and predicting the additional error given that the seed is incorrect. We adapt the generic DAER model to the problems of keypoint-conditioned viewpoint estimation and hierarchical scene classification, and show it outperforms strong baselines on both tasks.

Last, we show that DAER outperforms both of its components individually, including the mathematically equivalent task of regressing the additional error. Through an analysis of the sensitivity of the task model to incorrect seeds, we find evidence suggesting that the significant number of seeds that do not cause any additional error leads to

a strongly zero-biased training signal. Asking the model to first answer the easier question of whether or not the seed is correct ideally allows all of the correct seeds to be accepted first, while the additional error regression receives a more balanced training signal for rejecting seeds which are incorrect.

Seed rejection addresses a large number of problems which, up to this point, have assumed that seeds are correct. We offer a generic formulation of both the seed rejection problem and a solution, which we hope will be extended to more problems in future work.

Acknowledgements Toyota Research Institute ("TRI") provided funds to assist the authors with their research, but this article solely reflects the opinions and conclusions of its authors and not TRI or any other Toyota entity.

References

- [1] Stanislaw Antol, Aishwarya Agrawal, Jiasen Lu, Margaret Mitchell, Dhruv Batra, C. Lawrence Zitnick, and Devi Parikh. VQA: Visual Question Answering. In *2015 IEEE International Conference on Computer Vision (ICCV)*, pages 2425–2433, Santiago, Chile, Dec. 2015. IEEE.
- [2] Mohamed El Banani and Jason J. Corso. Adviser Networks: Learning What Question to Ask for Human-In-The-Loop Viewpoint Estimation. *arXiv:1802.01666 [cs]*, Oct. 2018. arXiv: 1802.01666.
- [3] Steve Branson, Catherine Wah, Florian Schroff, Boris Babenko, Peter Welinder, Pietro Perona, and Serge Belongie. Visual Recognition with Humans in the Loop. In *European Conference on Computer Vision*, volume 6314, pages 438–451, Berlin, Heidelberg, 2010. Springer Berlin Heidelberg.
- [4] C. Chow. On optimum recognition error and reject tradeoff. *IEEE Transactions on Information Theory*, 16(1):41–46, Jan. 1970.
- [5] Jia Deng, Wei Dong, Richard Socher, Li-Jia Li, Kai Li, and Li Fei-Fei. ImageNet: A Large-Scale Hierarchical Image Database. page 8, 2009.
- [6] Samuel Dodge and Lina Karam. Understanding How Image Quality Affects Deep Neural Networks. *arXiv:1604.04004 [cs]*, Apr. 2016. arXiv: 1604.04004.
- [7] Kevin Eykholt, Ivan Evtimov, Earlene Fernandes, Bo Li, Amir Rahmati, Chaowei Xiao, Atul Prakash, Tadayoshi Kohno, and Dawn Song. Robust Physical-World Attacks on Deep Learning Visual Classification. In *2018 IEEE/CVF Conference on Computer Vision and Pattern Recognition*, pages 1625–1634, Salt Lake City, UT, USA, June 2018. IEEE.
- [8] Giorgio Fumera and Fabio Roli. Support Vector Machines with Embedded Reject Option. In Gerhard Goos, Juris Hartmanis, Jan van Leeuwen, Seong-Whan Lee, and Alessandro Verri, editors, *Pattern Recognition with Support Vector Machines*, volume 2388, pages 68–82. Springer Berlin Heidelberg, Berlin, Heidelberg, 2002.
- [9] Yarin Gal. *Uncertainty in Deep Learning*. PhD thesis, 2016.
- [10] Yarin Gal and Zoubin Ghahramani. Dropout as a Bayesian Approximation: Representing Model Uncertainty in Deep Learning. page 10, 2016.
- [11] Yonatan Geifman and Ran El-Yaniv. Selective Classification for Deep Neural Networks. In *Advances in Neural Information Processing Systems*, pages 4878–4887, 2017.
- [12] Yonatan Geifman and Ran El-Yaniv. SelectiveNet: A Deep Neural Network with an Integrated Reject Option. *arXiv:1901.09192 [cs, stat]*, Jan. 2019. arXiv: 1901.09192.
- [13] Yonatan Geifman, Guy Uziel, and Ran El-Yaniv. Bias-Reduced Uncertainty Estimation for Deep Neural Classifiers. *arXiv:1805.08206 [cs, stat]*, May 2018. arXiv: 1805.08206.
- [14] Brent Griffin, Victoria Florence, and Jason J. Corso. Video Object Segmentation-based Visual Servo Control and Object Depth Estimation on a Mobile Robot Platform. *arXiv:1903.08336 [cs]*, Mar. 2019. arXiv: 1903.08336.
- [15] Brent A Griffin and Jason J Corso. BubbleNets: Learning to Select the Guidance Frame in Video Object Segmentation by Deep Sorting Frames. page 10.
- [16] Danna Gurari, Suyog Dutt Jain, Margrit Betke, and Kristen Grauman. Pull the Plug? Predicting If Computers or Humans Should Segment Images. In *2016 IEEE Conference on Computer Vision and Pattern Recognition (CVPR)*, pages 382–391, Las Vegas, NV, USA, June 2016. IEEE.
- [17] Kaiming He, Xiangyu Zhang, Shaoqing Ren, and Jian Sun. Deep Residual Learning for Image Recognition. *arXiv:1512.03385 [cs]*, Dec. 2015. arXiv: 1512.03385.
- [18] M. E. Hellman. The Nearest Neighbor Classification Rule with a Reject Option. *IEEE Transactions on Systems Science and Cybernetics*, 6(3):179–185, July 1970.
- [19] Hexiang Hu, Guang-Tong Zhou, Zhiwei Deng, Zicheng Liao, and Greg Mori. Learning Structured Inference Neural Networks with Label Relations. In *2016 IEEE Conference on Computer Vision and Pattern Recognition (CVPR)*, pages 2960–2968, Las Vegas, NV, USA, June 2016. IEEE.
- [20] Ronghang Hu, Marcus Rohrbach, and Trevor Darrell. Segmentation from Natural Language Expressions. *arXiv:1603.06180 [cs]*, Mar. 2016. arXiv: 1603.06180.
- [21] Jia-Bin Huang, Sing Bing Kang, Narendra Ahuja, and Johannes Kopf. Temporally coherent completion of dynamic video. *ACM Transactions on Graphics*, 35(6):1–11, Nov. 2016.
- [22] Panagiotis G. Ipeirotis, Foster Provost, and Jing Wang. Quality management on Amazon Mechanical Turk. In *Proceedings of the ACM SIGKDD Workshop on Human Computation - HCOMP '10*, page 64, Washington DC, 2010. ACM Press.
- [23] Justin Johnson, Lamberto Ballan, and Li Fei-Fei. Love Thy Neighbors: Image Annotation by Exploiting Image Metadata. In *2015 IEEE International Conference on Computer Vision (ICCV)*, pages 4624–4632, Santiago, Chile, Dec. 2015. IEEE.
- [24] Michal Koperski, Tomasz Konopczynski, Rafal Nowak, Piotr Semberecki, and Tomasz Trzcinski. Plugin Networks for Inference under Partial Evidence. *The IEEE Winter Conference on Applications of Computer Vision*, pages 2883–2891, 2020.

- [25] Matej Kristan, Jiri Matas, Ale Leonardis, Tom Voj, Roman Pflugfelder, Gustavo Fernandez, Georg Nebehay, Fatih Porikli, and Luka ehovin. A Novel Performance Evaluation Methodology for Single-Target Trackers. *IEEE Transactions on Pattern Analysis and Machine Intelligence*, 38(11):2137–2155, Nov. 2016.
- [26] Pierre M. Larochelle, Andrew P. Murray, and Jorge Angeles. A Distance Metric for Finite Sets of Rigid-Body Displacements via the Polar Decomposition. *Journal of Mechanical Design*, 129(8):883–886, Aug. 2007.
- [27] Jordi Pont-Tuset, Federico Perazzi, Sergi Caelles, Pablo Arbelaz, Alex Sorkine-Hornung, and Luc Van Gool. The 2017 DAVIS Challenge on Video Object Segmentation. *arXiv:1704.00675 [cs]*, Mar. 2018. arXiv: 1704.00675.
- [28] Vikas C Raykar and Shipeng Yu. Eliminating Spammers and Ranking Annotators for Crowdsourced Labeling Tasks. *Journal of Machine Learning Research*, 13:28, Feb. 2012.
- [29] N Dinesh Reddy, Minh Vo, and Srinivasa G. Narasimhan. CarFusion: Combining Point Tracking and Part Detection for Dynamic 3D Reconstruction of Vehicles. In *2018 IEEE/CVF Conference on Computer Vision and Pattern Recognition*, pages 1906–1915, Salt Lake City, UT, USA, June 2018. IEEE.
- [30] Amir Rosenfeld, Richard Zemel, and John K. Tsotsos. The Elephant in the Room. *arXiv:1808.03305 [cs]*, Aug. 2018. arXiv: 1808.03305.
- [31] Jeffrey M. Rzeszutarski and Aniket Kittur. Instrumenting the crowd: using implicit behavioral measures to predict task performance. In *Proceedings of the 24th annual ACM symposium on User interface software and technology - UIST '11*, page 13, Santa Barbara, California, USA, 2011. ACM Press.
- [32] Jean Y. Song, Raymond Fok, Alan Lundgard, Fan Yang, Juho Kim, and Walter S. Lasecki. Two Tools are Better Than One: Tool Diversity as a Means of Improving Aggregate Crowd Performance. In *Proceedings of the 2018 Conference on Human Information Interaction & Retrieval - IUI 18*, pages 559–570, Tokyo, Japan, 2018. ACM Press.
- [33] Jean Y. Song, Stephan J. Lemmer, Michael Xieyang Liu, Shiyang Yan, Juho Kim, Jason J. Corso, and Walter S. Lasecki. Popup: reconstructing 3D video using particle filtering to aggregate crowd responses. In *Proceedings of the 24th International Conference on Intelligent User Interfaces - IUI '19*, pages 558–569, Marina del Ray, California, 2019. ACM Press.
- [34] Hao Su, Charles R. Qi, Yangyan Li, and Leonidas J. Guibas. Render for CNN: Viewpoint Estimation in Images Using CNNs Trained with Rendered 3D Model Views. In *2015 IEEE International Conference on Computer Vision (ICCV)*, pages 2686–2694, Santiago, Chile, Dec. 2015. IEEE.
- [35] Christian Szegedy, Wojciech Zaremba, Ilya Sutskever, Joan Bruna, Dumitru Erhan, Ian Goodfellow, and Rob Fergus. Intriguing properties of neural networks. *arXiv:1312.6199 [cs]*, Feb. 2014. arXiv: 1312.6199.
- [36] Ryan Szeto and Jason J. Corso. Click Here: Human-Localized Keypoints as Guidance for Viewpoint Estimation. In *2017 IEEE International Conference on Computer Vision (ICCV)*, pages 1604–1613, Venice, Oct. 2017. IEEE.
- [37] Shubham Tulsiani and Jitendra Malik. Viewpoints and keypoints. In *2015 IEEE Conference on Computer Vision and Pattern Recognition (CVPR)*, pages 1510–1519, Boston, MA, USA, June 2015. IEEE.
- [38] Igor Vasiljevic, Ayan Chakrabarti, and Gregory Shakhnarovich. Examining the Impact of Blur on Recognition by Convolutional Networks. *arXiv:1611.05760 [cs]*, May 2017. arXiv: 1611.05760.
- [39] Tianlu Wang, Kota Yamaguchi, and Vicente Ordonez. Feedback-Prop: Convolutional Neural Network Inference Under Partial Evidence. In *2018 IEEE/CVF Conference on Computer Vision and Pattern Recognition*, pages 898–907, Salt Lake City, UT, June 2018. IEEE.
- [40] Rey Reza Wiyatno and Anqi Xu. Physical Adversarial Textures that Fool Visual Object Tracking. *arXiv:1904.11042 [cs]*, Sept. 2019. arXiv: 1904.11042.
- [41] Zuxuan Wu, Ser-Nam Lim, Larry Davis, and Tom Goldstein. Making an Invisibility Cloak: Real World Adversarial Attacks on Object Detectors. *arXiv:1910.14667 [cs, math]*, Oct. 2019. arXiv: 1910.14667.
- [42] Yu Xiang, Roozbeh Mottaghi, and Silvio Savarese. Beyond PASCAL: A benchmark for 3D object detection in the wild. In *IEEE Winter Conference on Applications of Computer Vision*, pages 75–82, Steamboat Springs, CO, USA, Mar. 2014. IEEE.
- [43] Mehmet Yigit Yildirim, Mert Ozer, and Hasan Davulcu. Leveraging Uncertainty in Deep Learning for Selective Classification. *arXiv:1905.09509 [cs, math, stat]*, May 2019. arXiv: 1905.09509.
- [44] Yiren Zhou, Sibong Song, and Ngai-Man Cheung. On classification of distorted images with deep convolutional neural networks. In *2017 IEEE International Conference on Acoustics, Speech and Signal Processing (ICASSP)*, pages 1213–1217, New Orleans, LA, Mar. 2017. IEEE.